Computers and Mathematics with Applications 66 (2013) 1104–1119

Contents lists available at ScienceDirect

Computers and Mathematics with Applications

journal homepage: www.elsevier.com/locate/camwa

Adjoint method for a tumor growth PDE-constrained optimization problem

D.A. Knopoff*, D.R. Fernández, G.A. Torres, C.V. Turner

Facultad de Matemática, Astronomía y Física, Medina Allende s/n, 5000 Córdoba, Argentina
Centro de Investigaciones y Estudios en Matemática - CONICET, Medina Allende s/n, 5000 Córdoba, Argentina

ARTICLE INFO

Article history:
Received 19 March 2012
Received in revised form 26 February 2013
Accepted 8 May 2013

Keywords:
Avascular tumor
PDE-constrained optimization
Inverse problem
Mathematical modeling
Adjoint method

ABSTRACT

In this paper we present a method for estimating unknown parameters that appear on an avascular, spheric tumor growth model. The model for the tumor is based on nutrient driven growth of a continuum of live cells, whose birth and death generate volume changes described by a velocity field. The model consists of a coupled system of partial differential equations whose spatial domain is the tumor, that changes in size over time. Thus, the situation can be formulated as a free boundary problem. After solving the direct problem properly, we use the model for the estimation of parameters by fitting the numerical solution with real data, obtained via *in vitro* experiments and medical imaging. We define an appropriate functional to compare both the real data and the numerical solution. We use the adjoint method for the minimization of this functional.

1. Introduction

The interest in research for modeling cancer has grown enormously over the last years, for example [1,2] which focus on computational methods for simulations, and [3–5] which show how the properties of biological tissues evolve in time. It has become one of the most challenging topics involving applied mathematicians working with researchers in the biological sciences. One of the main motivations is the fact that, according to the World Health Organization, about six million people die annually because of cancer, the second main fatal disease in industrialized countries.

Key comments on the importance of mathematical modeling on cancer can be found in a vast array of literature. For example, in the work by Bellomo et al. [5], they emphasize the fact that "applied mathematics may be able to provide a framework in which experimental results can be interpreted, and a quantitative analysis of external actions to control neoplastic growth can be developed". Moreover, "models and simulations can reduce the amount of experimentation necessary for drug and therapy development".

Some developments in the last years include, among many others, cell-focused [6], hybrid [7,8] and continuum models [9], each of them with some specific fields of applications.

In this paper we consider the case of avascular multicellular spheroids (MCS). Pioneers in this subject have been, for example [10,11], where the first spatio-temporal models of MCS' growth have been developed. The study of MCS is interesting because they provide the best insight into the effects of varying nutrient concentrations or the effectiveness of chemotherapeutic drugs on tumors *in vivo*, and their behavior can be studied experimentally (*in vitro*) by controlling environmental conditions in which they grow: for example, the radii of the tumor can be monitored while changing the chemotherapeutic drug or oxygen levels.

* Corresponding author at: Facultad de Matemática, Astronomía y Física, Medina Allende s/n, 5000 Córdoba, Argentina.
E-mail addresses: knopoff@famaf.unc.edu.ar, damianknopoff@gmail.com (D.A. Knopoff), dfernandez@famaf.unc.edu.ar (D.R. Fernández), torres@famaf.unc.edu.ar (G.A. Torres), turner@famaf.unc.edu.ar (C.V. Turner).

0898-1221/$ – see front matter © 2013 Elsevier Ltd. All rights reserved.
http://dx.doi.org/10.1016/j.camwa.2013.05.028

In addition, other variables can be measured. If possible, experimentalists can get information about the distribution of substances within the tumor. Moreover, via medical imaging, histopathology and potentially other sources, they can also get data about the density of the different kind of cells conforming it: proliferating, quiescent, necrotic. For instance, as documented in [12] the Boron Neutron Capture Therapy (BNCT) technique gives information about the evolution in size of a melanoma, and in [13], they obtain information about the growth of a glioma via Magnetic Resonance Imaging (MRI).

That is why in this general approach of modeling, the key variables are the tumor size (radius), the concentration within the tumor of growth-rate limiting diffusible chemicals (nutrients such as oxygen or glucose or a chemotherapeutic drug) and the density of cells. Since the tumor changes in size over time, the domain on which the models are formulated must be determined as a part of the solution process, giving a vast class of moving boundary problems [14,15].

In this article, we propose a framework for estimating unknown parameters via a PDE-constrained optimization problem, following the PDE-based model by Ward and King [16], which is a two phase model with the two phases being live cells and dead cells. This model is, to our knowledge, the first one in which the spatial structure of avascular tumors does not assume distinct cell layers and one of its main advantages is that it accurately reproduces the early stages of a spheroid's growth in a quite simple way. However, it is worth stressing that some extensions have been done [17–19] and many improvements can be considered from a biological point of view (for instance, vascularization and symmetry breaking).

This kind of problem constitutes a particular application of the so-called inverse problems, which are being increasingly used in a broad number of fields in applied sciences. For example, problems referred to structured population dynamics [20], computerized tomography and image reconstruction in medical imaging [21,22], and more specifically tumor growth [23,13], among many others.

In a previous work [24, unpublished work] the authors solved an inverse problem using a Pattern Search algorithm to obtain the efficiency of a drug. In this paper we are concerned with developing a robust PDE-constrained formulation that let us find the best set of parameters of a tumor growth model that fits patient or experimental data. We want to find the parameters that would be of interest by defining a functional to be minimized. In contrast to the previous work, in which we used a free-derivative method, we now use the adjoint method in order to find the derivative of the functional to be minimized. Since Pattern Search methods require a number of functional evaluations that grows with the number of parameters to be retrieved, they are not convenient for a multidimensional parameter space. That is the reason why we prefer a gradient-based method.

The contents of this paper, which is organized into 7 sections, are as follows: Section 2 consists of some preliminaries about the model and the definition of the direct problem. Section 3 deals with the motivation and formulation of the minimization problem. Section 4 introduces the adjoint problem, deriving the optimality conditions for the problem. Specifically, we show how the adjoint method may be used to find the derivative of the solution of a PDE with respect to a parameter that does not appear explicitly in the equation. Section 5 refers to the resolution of the adjoint and reduced problems. In particular, we develop a method to deal with some singularities in the PDEs, and it deals with the minimization method to be used. In Section 6 we show some numerical simulations to give information on the behavior of the functional and its dependence on the parameters. Section 7 presents the conclusions and introduces some future work related to the contents of this paper.

Some words about our notation. We use $\langle\cdot,\cdot\rangle$ to denote the L^2 inner product (the space is always clear from the context) and we consider the sum of inner products for a Cartesian product of spaces. For a function $F : \mathcal{Y} \times \mathcal{U} \to \mathcal{Z}$ such that $(\phi, p) \mapsto F(\phi, p)$, we denote by $F'(\phi, p)$ the full Fréchet-derivative and by $\frac{\partial F}{\partial \phi}(\phi, p)$ and $\frac{\partial F}{\partial p}(\phi, p)$ the partial Fréchet-derivatives of F at (ϕ, p). For a linear operator $T : \mathcal{Y} \to \mathcal{Z}$ we denote $T^* : \mathcal{Z}^* \to \mathcal{Y}^*$ the adjoint operator of T. If T is invertible, we call T^{-*} the inverse of the adjoint operator T^*.

2. Some preliminaries about the model

We consider the model proposed in [16] where the resolution of a coupled system of spatio-temporal PDEs involving initial and boundary conditions is discussed, with the additional difficulty that the boundary is also an unknown. In that work the tumor is considered to be a spheroid consisting of a continuum of living cells, in one of two states: live or dead. The rates of birth and death depend on the nutrient. It is supposed that those processes generate volume changes, leading to cell movement described by a velocity field. Under this assumption, the system of equations to be studied is:

$$\frac{\partial \eta}{\partial t} + \frac{1}{r^2}\frac{\partial (r^2 \nu \eta)}{\partial r} = [k_m(\varsigma, \theta) - k_d(\varsigma, \theta)]\eta, \tag{1}$$

$$\frac{\partial \varsigma}{\partial t} + \frac{1}{r^2}\frac{\partial (r^2 \nu \varsigma)}{\partial r} = \frac{D}{r^2}\frac{\partial}{\partial r}\left(r^2 \frac{\partial \varsigma}{\partial r}\right) - \beta k_m(\varsigma, \theta)\eta, \tag{2}$$

$$\frac{1}{r^2}\frac{\partial (r^2 \nu)}{\partial r} = [V_L k_m(\varsigma, \theta) - (V_L - V_D)k_d(\varsigma, \theta)]\eta, \tag{3}$$

where the dependent variables η, ς and ν are the live cell density (cells/unit volume), nutrient concentration and velocity, respectively. The independent variables are the radial position r inside the tumor and time t. Constants V_L and V_D correspond to the volume of a living and a death cell, respectively. The number D is the diffusion coefficient of the nutrient and β is a

positive constant related to the nutrient's consumption rate. As it is described in [16], Eq. (1) states that the rate of change of η is dependent on the difference between the birth $k_m(\varsigma, \theta)$ and death $k_d(\varsigma, \theta)$ rates (θ is a vector of parameters associated to these functions). The functions k_m and k_d are taken to be generalized Michaelis–Menten kinetics with exponent 1, i.e.,

$$k_m(\varsigma, \theta) = A\left(\frac{\varsigma}{\varsigma_c + \varsigma}\right), \tag{4}$$

$$k_d(\varsigma, \theta) = B\left(1 - \sigma\frac{\varsigma}{\varsigma_d + \varsigma}\right), \tag{5}$$

with $\theta = [A, B, \varsigma_c, \varsigma_d, \sigma]^T$ where A and B are the maximum birth and death rates theoretically attainable when ς tends to infinity and $\varsigma = 0$ respectively, the constants ς_c and ς_d are the standard half-saturation concentrations in the Michaelis–Menten terms, and $B(1-\sigma)$ is the minimum death rate attainable when the concentration tends to infinity with $0 \leq \sigma \leq 1$. As stated in the appendix of [16], there appears to be no appropriate data available on the parameters ς_d and σ, constituting one extra motivation for this work.

Inherent in this problem are two timescales: the tumor growth timescale ($\approx$1 day) and the much shorter nutrient diffusion ($\approx$1 min), letting us to adopt a quasisteady assumption in the nutrient equation (see [16]). Therefore, we replace (2) by the quasisteady approximation

$$\frac{1}{r^2}\frac{\partial}{\partial r}\left(r^2\frac{\partial \varsigma}{\partial r}\right) = \frac{\beta}{D}k_m(\varsigma, \theta)\eta. \tag{6}$$

As it was mentioned in [25], the model proposed by Ward and King [16] has made significant contributions on avascular tumor growth. One of the advantages of this model is that it does not appeal to the theory of porous media and the theory of mixtures, and it uses a generalized Michaelis–Menten form for the rate constants for cell proliferation and death.

2.1. Initial and boundary conditions

As it has been mentioned, the tumor is assumed to be a spheroid that exhibits radial symmetry. That is why, not only are the state variables η, ς and ν important, but also the tumor radius is a key variable to be determined. Since the tumor changes in size over time, the domain on which the model is formulated (and the PDEs are valid) must be determined as part of the solution.

Let $\mathcal{S}(t)$ be the tumor radius at time t. At $t = 0$ we will consider the tumor at a certain stage of its evolution. Hence the initial conditions are a known radius $\mathcal{S}(0)$ and an initial live cell density

$$\eta(r, 0) = \eta_I(r).$$

Because symmetry is assumed about the tumor center, there is no flux there. That is why the boundary conditions at $r = 0$ are:

$$\frac{\partial \varsigma}{\partial r}(0, t) = 0, \tag{7}$$

$$\nu(0, t) = 0. \tag{8}$$

Moreover, on the external boundary (which is also the boundary of the complement of the tumor as a subset of the body), the following conditions are taken:

$$\varsigma(\mathcal{S}(t), t) = c_0, \tag{9}$$

$$\frac{d\mathcal{S}}{dt} = \nu(\mathcal{S}(t), t), \tag{10}$$

where c_0 is the external nutrient concentration.

2.2. Nondimensionalization and fixed domain method

Following the ideas exposed in [26,27,14,16,17], the mathematical model is rescaled and the domain $[0, \mathcal{S}(t)]$ of the tumor is transformed onto the interval [0, 1]. This is a very useful approach when dealing with free-boundary problems, as mentioned in [15]. Hence, let us define the following functions

$$N(y, t) = V_L\eta(y\mathcal{S}(t/A), t/A),$$

$$C(y, t) = \frac{1}{c_0}\varsigma(y\mathcal{S}(t/A), t/A),$$

$$V(y, t) = \frac{1}{Ar_0}\nu(y\mathcal{S}(t/A), t/A),$$

$$S(t) = \frac{1}{r_0}\mathcal{S}(t/A),$$
$$a(c,\vartheta) = \frac{1}{A}[k_m(c,\vartheta) - k_d(c,\vartheta)],$$
$$b(c,\vartheta) = \frac{1}{A}[k_m(c,\vartheta) - (1-\delta)k_d(c,\vartheta)],$$
$$k(c,\vartheta) = \widehat{\beta}k_m(c,\vartheta),$$

where $r_0 = (3V_L/4\pi)^{1/3}$ is the radius of a single cell, $\delta = V_D/V_L$, $\widehat{\beta} = r_0^2\beta/(V_L c_0 D)$ and $\vartheta = [A, B, c_c, c_d, \sigma]$ with $c_c = \varsigma_c/c_0$ and $c_d = \varsigma_d/c_0$. Thus, we obtain the following system to be solved:

$$N_t - \frac{S'}{S}yN_y + \frac{V}{S}N_y = N[a(C,\vartheta) - b(C,\vartheta)N], \quad 0 < y \le 1,\ t > 0, \tag{11}$$

$$C_{yy} + \frac{2}{y}C_y = k(C,\vartheta)S^2N, \quad 0 < y \le 1,\ t > 0, \tag{12}$$

$$V_y + \frac{2}{y}V = b(C,\vartheta)NS, \quad 0 < y \le 1,\ t > 0. \tag{13}$$

The initial conditions for the transformed problem are:

$$N(y,0) = N_I(y), \quad 0 \le y \le 1, \tag{14}$$
$$S(0) = S_I, \tag{15}$$

where $N_I(y) = V_L\eta_I(y\mathcal{S}(0),0)$ and $S_I = \mathcal{S}(0)/r_0$, and the boundary conditions are:

$$V(0,t) = 0, \quad t > 0, \tag{16}$$
$$C_y(0,t) = 0, \quad t > 0, \tag{17}$$
$$C(1,t) = 1, \quad t > 0, \tag{18}$$
$$S'(t) = V(1,t), \quad t > 0. \tag{19}$$

From now on, Eqs. (11)–(19) will be referred to as the direct problem.

3. Formulation of the minimization problem

As described above, there is a set of parameters (some of them unknown) that determines the behavior of a tumor's growth. For this reason we propose to use an inverse problem technique in order to estimate them.

We define the following vectors:

$$\phi = [N, V, C, S]^T, \tag{20}$$
$$p = [c_c, c_d, \sigma]^T, \tag{21}$$

where ϕ represents the solution of the direct problem (the components of ϕ are the state variables of the problem) for each choice of the vector of parameters $\vartheta = (A, B, p)$, where A and B are assumed to be constants. Hence from now on, we will use just p instead of ϑ as the vector of parameters.

Let us assume that experimental information is available during the time interval $0 \le t \le T$. Then, the general problem we are interested in solving can be formulated as:

Find a parameter p able to generate data $\phi = [N, C, V, S]^T$ *that best match the available* (*experimental*) *information over time* $0 \le t \le T$.

For this purpose, we should construct an objective function which gives us a notion of distance between the experimental (real) data and the solution of the system of PDEs for each choice of parameters p.

First of all, it is important to decide which variables are measurable experimentally. For instance, it is clear that the tumor radius can be known at certain times $t_k,\ k = 1, \ldots, M$ via MRI, PET (Positron Emission Tomography) or CT (Computed Tomography). For example, Fig. 1 is a microscopic field that shows the formation *in vitro* of neoplastic colonies which grow as spheroids with an external nutrient supply. Such experiments could help to determine optimal variables and parameters in order to control real tumor growth.

So, the first possibility for defining a functional could be:

$$J(S,p) = \frac{1}{2}\int_0^T [S(t) - S^*(t)]^2 dt,$$

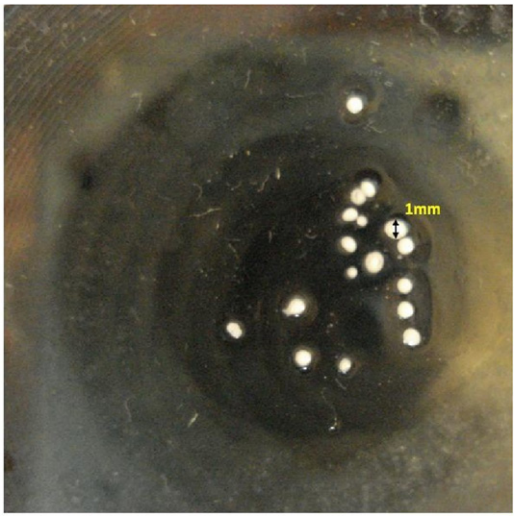

Fig. 1. Microscopic image of neoplastic colonies that grow with an external nutrient supply. *Courtesy of CNEA (Comisión Nacional de Energía Atómica).*

where $S(t)$ is the radius evolution obtained by solving the direct problem for a certain choice of p and $S^*(t) = \frac{1}{r_0}\mathcal{S}^*(t/A)$ is the evolution measured experimentally (real data).

Another variable that could be measured is the density of living cells, also via biomedical imaging. As it was mentioned before, this could be done via PET technique for a tumor *in vivo*, or via immunofluorescence and electronic scan microscopy technique for *in vitro* cases [28,29]. Thus, we are motivated to define a functional that reproduces in a better way the knowledge we have about the process.

For instance, in [30], the mean size of a spheroid population was determined by measuring two orthogonal diameters on spheroids using an inverted microscope fitted with a calibrated eyepiece reticule; in [31,32] a special procedure was used with digital microscope photos to evaluate tumor growth; in [33] spheroids were photographed in an inverted phase contrast microscope while a micrometer scale was photographed at the same magnification, and spheroid size was determined.

$$J(N, S, p) = \frac{\mu_1}{2}\int_0^1\int_0^T [N(y,t) - N^*(y,t)]^2 dtdy + \frac{\mu_2}{2}\int_0^T [S(t) - S^*(t)]^2 dt, \tag{22}$$

where $N(y,t)$ and $N^*(y,t)$ are the living cell concentrations for the direct problem solved with the parameters p and the real data, respectively (both of them in the domain $[0,1]\times[0,T]$). The positive constants μ_1 and μ_2 are introduced, as we shall see, to take into account the different order of magnitude between N and S. Note that, for instance, if we take $\mu_1 = 0$ and $\mu_2 = 1$ in (22) we get the previous functional. In this way, these two parameters will give us some flexibility in order to choose an appropriate functional according to the experimental method used to obtain the data.

It should be noted that the spatial integration is done over the interval $[0,1]$, because we are using the solution in the fixed domain.

Let us define

$$E(\phi, p) = \begin{bmatrix} N_t - N_y\dfrac{S'}{S}y + \dfrac{V}{S}N_y - N\left(a(C,p) - b(C,p)N\right) \\ V_y + \dfrac{2}{y}V - b(C,p)NS \\ C_{yy} + \dfrac{2}{y}C_y - k(C,p)NS^2 \\ V(1,\cdot) - S' \\ V(0,\cdot) \\ C(1,\cdot) - 1 \\ C_y(0,\cdot) \\ N(\cdot,0) - N_I \\ S(0) - S_I \end{bmatrix}. \tag{23}$$

In this way we can rewrite the system of PDEs (11)–(19) described in the previous section as $E(\phi, p) = 0$.

The set of parameters that best matches the experimental data with the generated data provided by the direct problem can be computed solving a PDE-constrained optimization problem, namely:

$$\begin{aligned} &\underset{p}{\text{minimize}} && J(\phi, p) \\ &\text{subject to} && E(\phi, p) = 0, \\ &&& p \in U_{\text{ad}}, \end{aligned} \tag{24}$$

where U_{ad} denotes the set of admissible values of p. In our case, according to (21), U_{ad} should be a subset of $\mathbb{R}^3$. Notice that a solution (ϕ, p) must satisfy the constraints $E(\phi, p) = 0$, which constitute the direct problem.

We remark that, in general, there is a fundamental difference between the direct and the inverse problems. In fact, the latter is usually ill-posed in the sense of existence, uniqueness and stability of the solution. This inconvenience is often treated by using some regularization techniques [21,34,35], but in our case it was not necessary.

4. The adjoint problem

4.1. Formulation of the reduced and adjoint problems

In the following, we will consider a generic optimization problem, which has the form:

$$\begin{aligned} &\underset{p}{\text{minimize}} && J(\phi, p) \\ &\text{subject to} && E(\phi, p) = 0, \\ &&& p \in U_{\text{ad}}, \end{aligned} \tag{25}$$

where $J : \mathcal{Y} \times U_{\text{ad}} \to \mathbb{R}$ is an objective function and $E : \mathcal{Y} \times U_{\text{ad}} \to \mathcal{Z}$ is a state equation, for $\mathcal{Y}$ and $\mathcal{Z}$ Banach spaces and U_{ad} is a set of admissible points.

For completeness, in this section we will present a general theory in order to solve problem (25). According to the ideas exposed in [36,37], we make the following assumptions:

(A1) $U_{\text{ad}} \in \mathbb{R}^m$ is a nonempty, closed and convex set.
(A2) $J : \mathcal{Y} \times U_{\text{ad}} \to \mathbb{R}$ and $E : \mathcal{Y} \times U_{\text{ad}} \to \mathcal{Z}$ are continuously Fréchet-differentiable functions.
(A3) For each $p \in U_{\text{ad}}$ there exists a unique corresponding solution $\phi(p) \in \mathcal{Y}$ such that $E(\phi(p), p) = 0$. Thus, there is a *unique solution operator* $p \in U_{\text{ad}} \mapsto \phi(p) \in \mathcal{Y}$.
(A4) The derivative $\frac{\partial E}{\partial \phi}(\phi(p), p) : \mathcal{Y} \to \mathcal{Z}$ is a continuous linear operator, and it is continuously invertible for all $p \in U_{\text{ad}}$.

Under these hypotheses $\phi(p)$ is continuously differentiable on $p \in U_{\text{ad}}$ by the implicit function theorem. Thus, it is reasonable to define the following so-called reduced problem

$$\begin{aligned} &\underset{p}{\text{minimize}} && \tilde{J}(p) = J(\phi(p), p) \\ &\text{subject to} && p \in U_{\text{ad}}, \end{aligned} \tag{26}$$

where $\phi(p)$ is given as the solution of $E(\phi(p), p) = 0$.

In order to find a minimum of the continuously differentiable function $\tilde{J}$, it will be important to compute the derivative of this reduced objective function. Hence, we will show a procedure to obtain $\tilde{J}'$ by using the adjoint approach. Since

$$\begin{aligned} \left\langle \tilde{J}'(p), q \right\rangle &= \left\langle \frac{\partial J}{\partial \phi}(\phi(p), p), \phi'(p)q \right\rangle + \left\langle \frac{\partial J}{\partial p}(\phi(p), p), q \right\rangle \\ &= \left\langle \left(\phi'(p)\right)^* \frac{\partial J}{\partial \phi}(\phi(p), p) + \frac{\partial J}{\partial p}(\phi(p), p), q \right\rangle \end{aligned}$$

we see that

$$\tilde{J}'(p) = \left(\phi'(p)\right)^* \frac{\partial J}{\partial \phi}(\phi(p), p) + \frac{\partial J}{\partial p}(\phi(p), p). \tag{27}$$

Let us consider $\lambda \in \mathcal{Z}^*$ as the solution of the so-called adjoint problem:

$$\frac{\partial J}{\partial \phi}(\phi(p), p) + \left(\frac{\partial E}{\partial \phi}(\phi(p), p)\right)^* \lambda = 0 \tag{28}$$

where $\left(\frac{\partial E}{\partial \phi}(\phi, p)\right)^*$ is the adjoint operator of $\frac{\partial E}{\partial \phi}(\phi, p)$. Note that each term in (28) is an element of the space $\mathcal{Y}^*$.

An equation for the derivative $\phi'(p)$ is obtained by differentiating the equation $E(\phi(p), p) = 0$ with respect to p:

$$\frac{\partial E}{\partial \phi}(\phi(p), p)\phi'(p) + \frac{\partial E}{\partial p}(\phi(p), p) = 0, \tag{29}$$

where 0 is the zero vector in $\mathcal{Z}$.

By using (27) we have that:

$$\begin{aligned}\tilde{J}'(p) &= \left(\phi'(p)\right)^* \frac{\partial J}{\partial \phi}(\phi(p), p) + \frac{\partial J}{\partial p}(\phi(p), p) \\ &= -\left(\frac{\partial E}{\partial p}(\phi(p), p)\right)^* \left(\frac{\partial E}{\partial \phi}(\phi(p), p)\right)^{-*} \frac{\partial J}{\partial \phi}(\phi(p), p) + \frac{\partial J}{\partial p}(\phi(p), p) \\ &= \left(\frac{\partial E}{\partial p}(\phi(p), p)\right)^* \lambda + \frac{\partial J}{\partial p}(\phi(p), p),\end{aligned}$$

where in the second equation we used (29) and for the last equation we used (28). Then:

$$\tilde{J}'(p) = \frac{\partial J}{\partial p}(\phi(p), p) + \left(\frac{\partial E}{\partial p}(\phi(p), p)\right)^* \lambda. \tag{30}$$

Notice that in order to obtain $\tilde{J}'(p)$ we need first to compute $\phi(p)$ by solving the direct problem, followed by the calculation of λ by solving the adjoint problem. For computing the second term of (30) it is not necessary to obtain the adjoint of $\frac{\partial E}{\partial p}(\phi(p), p)$ but just its action over λ.

4.2. Getting the adjoint equation for the concrete problem

For our case, let us define $\Omega = [0, 1] \times [0, T]$, the spatio-temporal domain of interest. Note that, according to (20), ϕ is an element of a suitable vector space. Let us consider the function spaces

$$\begin{aligned}\mathcal{Y} &= \left(\mathcal{C}^1(\Omega)\right)^2 \times \mathcal{C}^2(\Omega) \times \mathcal{C}^1([0, T]), \\ \mathcal{Z} &= \left(\mathcal{C}^1(\Omega)\right)^2 \times \mathcal{C}^2(\Omega) \times \left(\mathcal{C}^1([0, T])\right)^4 \times \mathcal{C}([0, 1]) \times \mathbb{R}.\end{aligned}$$

The spaces $\mathcal{C}^1$ and $\mathcal{C}^2$ inherit the inner product from L^2, so the completeness of the spaces $\mathcal{Y}$ and $\mathcal{Z}$ are Hilbert spaces (therefore we can identify $\mathcal{Y}^*$ and $\mathcal{Z}^*$ with $\mathcal{Y}$ and $\mathcal{Z}$ respectively). It is worth mentioning that we consider these vector spaces because we look for strong solutions of the PDEs, i.e., we require differentiability of the state variables.

In order to obtain the adjoint operator of $\frac{\partial E}{\partial \phi}$, we have to find $\left(\frac{\partial E}{\partial \phi}\right)^*$ such that:

$$\left\langle \lambda, \frac{\partial E}{\partial \phi} g \right\rangle = \left\langle \left(\frac{\partial E}{\partial \phi}\right)^* \lambda, g \right\rangle. \tag{31}$$

Hence, we define the directions n, v, c, and s for the state variables N, V, C and S. Let $g = [n, v, c, s]^T$, then

$$\frac{\partial E}{\partial \phi}(\phi, p) g = \lim_{\mu \to 0^+} \frac{E(\phi + \mu g, p) - E(\phi, p)}{\mu}.$$

After some algebraics, it can be shown that $\frac{\partial E}{\partial \phi}(\phi, p)\, g$ is given by:

$$\begin{bmatrix} n_t + \frac{V - yS'}{S} n_y - \frac{s'S - S's}{S^2} N_y y + N_y \frac{vS - Vs}{S^2} - (a - bN)n - N\left(\frac{\partial a}{\partial C} c - \frac{\partial b}{\partial C} Nc - bn\right) \\ v_y + \frac{2}{y} v - \frac{\partial b}{\partial C} NSc - bSn - bNs \\ c_{yy} + \frac{2}{y} c_y - kS^2 n - \frac{\partial k}{\partial C} NS^2 c - 2kNSs \\ v(1, \cdot) - s' \\ v(0, \cdot) \\ c(1, \cdot) \\ c_y(0, \cdot) \\ n(\cdot, 0) \\ s(0) \end{bmatrix}. \tag{32}$$

Note that $E(\phi, p)$ and λ should have the same number of components. Also, each component of λ must be in a subspace of the corresponding component of E. For example, the first three components of λ must depend on space and time, the fourth one only on time, the last one is just a real number, and so on.

So we define:

$$\lambda(y, t) = [\lambda_1(y, t), \lambda_2(y, t), \lambda_3(y, t), \lambda_4(t), \lambda_5(t), \lambda_6(t), \lambda_7(t), \lambda_8(y), \lambda_9]^T. \tag{33}$$

An inspection over Eqs. (31) and (32) shows that, roughly speaking, we should remove the spatial and temporal derivatives from g and *pass* them to λ. To achieve this goal, we shall obtain equivalent expressions for each of the nine terms of the summation $\langle \frac{\partial E}{\partial \phi} g, \lambda \rangle$. Denoting as $\frac{\partial E_i}{\partial \phi}$ the i-th component of (32), we have the following equivalences:

Constraint 1. Using integration by parts repeatedly and the facts that $V(1,t) = S'(t)$ and $V(0,t) = 0$, it yields

$$\begin{aligned}\iint_\Omega \frac{\partial E_1}{\partial \phi}\lambda_1 dtdy = &\iint_\Omega \left[-\lambda_{1t} - \left(\frac{V - yS'}{S}\right)\lambda_{1y} - \left(\frac{V_y - S'}{S} + a - 2bN\right)\lambda_1\right] n\, dtdy \\ &+ \iint_\Omega \frac{N_y}{S}\lambda_1 v\, dtdy - \iint_\Omega N\left(\frac{\partial a}{\partial C} - \frac{\partial b}{\partial C}N\right)\lambda_1 c\, dtdy \\ &+ \iint_\Omega \left(\frac{yN_{yt}}{S}\lambda_1 + \frac{yN_y}{S}\lambda_{1t} - \frac{N_y V}{S^2}\lambda_1\right) s\, dtdy \\ &+ \int_0^1 (\lambda_1(y,T)n(y,T) - \lambda_1(y,0)n(y,0))\, dy \\ &+ s(0)\int_0^1 \frac{yN_y(y,0)\lambda_1(y,0)}{S(0)}dy - s(T)\int_0^1 \frac{yN_y(y,T)\lambda_1(y,T)}{S(T)}dy. \end{aligned} \tag{34}$$

Constraint 2. In this case we have to integrate by parts just in the first term, because it is the only one that has a derivative of g, in this case v_y. So we obtain that the second term in the inner product is

$$\begin{aligned}\iint_\Omega \frac{\partial E_2}{\partial \phi}\lambda_2 dtdy = &\iint_\Omega \left[\left(-\lambda_{2y} + \frac{2}{y}\lambda_2\right) v - \frac{\partial b}{\partial C}NS\lambda_2 c - bS\lambda_2 n - bN\lambda_2 s\right] dtdy \\ &+ \int_0^T (\lambda_2(1,t)v(1,t) - \lambda_2(0,t)v(0,t))\, dt. \end{aligned} \tag{35}$$

Constraint 3. Because of the presence of second order derivatives we integrate by parts twice. In order to perform the calculations, we assume that $\lambda_3(y,t)c(y,t) \to 0$ when $y \to 0$. Applying l'Hôpital's rule, we get

$$\begin{aligned}\iint_\Omega \frac{\partial E_3}{\partial \phi}\lambda_3 dtdy = &\iint_\Omega \left\{\left[\lambda_{3yy} - \frac{2}{y}\lambda_{3y} + \left(\frac{2}{y^2} - \frac{\partial k}{\partial C}NS^2\right)\lambda_3\right] c - kS^2\lambda_3 n + 2kNS\lambda_3 s\right\} dtdy \\ &+ \int_0^T \left[2\lambda_3(1,t)c(1,t) + \lambda_3(1,t)c_y(1,t) - \lambda_{3y}(1,t)c(1,t)\right] dt \\ &- \int_0^T \left[3\lambda_3(0,t)c_y(0,t) + \lambda_{3y}(0,t)c(0,t)\right] dt. \end{aligned} \tag{36}$$

Constraint 4. Since there is just one derivative of g involved in the corresponding term, we integrate by parts obtaining

$$\int_0^T \frac{\partial E_4}{\partial \phi}\lambda_4 dt = \int_0^T [\lambda_4(t)v(1,t) + \lambda_{4t}(t)s(t)]\, dt - \lambda_4(T)s(T) + \lambda_4(0)s(0). \tag{37}$$

Constraint 5. Because this term is free of derivatives, there is nothing to do with it, remaining:

$$\int_0^T \frac{\partial E_5}{\partial \phi}\lambda_5 dt = \int_0^T \lambda_5(t)v(0,t)dt. \tag{38}$$

Constraint 6. In this case, again, the corresponding term in the inner product remains:

$$\int_0^T \frac{\partial E_6}{\partial \phi}\lambda_6 dt = \int_0^T \lambda_6(t)c(1,t)dt. \tag{39}$$

Constraint 7. Even though this term has the derivative c_y, it remains unchanged because function λ_7 depends only on time:

$$\int_0^T \frac{\partial E_7}{\partial \phi}\lambda_7 dt = \int_0^T \lambda_7(t)c_y(0,t)dt. \tag{40}$$

Constraint 8. Once more, because of the lack of derivatives the term remains unchanged:

$$\int_0^1 \frac{\partial E_8}{\partial \phi}\lambda_8 dy = \int_0^1 \lambda_8(y)n(y,0)dy. \tag{41}$$

Constraint 9. In this case, the term is just the product of two real numbers:

$$\frac{\partial E_9}{\partial \phi}\lambda_9 = \lambda_9 s(0). \tag{42}$$

Obtaining the adjoint equations. On the other hand, by (22) we have that

$$\frac{\partial J}{\partial \phi} g = \mu_1 \iint_\Omega [N(y,t) - N^*(y,t)] n(y,t) dt dy + \mu_2 \int_0^T [S(t) - S^*(t)] s(t) dt. \tag{43}$$

Recall that we have to find λ satisfying Eq. (28) which is equivalent to

$$0 = \left\langle \frac{\partial J}{\partial \phi} + \left(\frac{\partial E}{\partial \phi} \right)^* \lambda, g \right\rangle = \left\langle \frac{\partial J}{\partial \phi}, g \right\rangle + \left\langle \lambda, \frac{\partial E}{\partial \phi} g \right\rangle,$$

for any direction $g \in \mathcal{Y}$.

So, putting together Eqs. (43) with (34)–(42) and choosing the directions conveniently, we get the following system of equations which constitutes the adjoint problem:

$$-\lambda_{1_t} - \left(\frac{V - yS'}{S} \right) \lambda_{1_y} - \left(\frac{V_y - S'}{S} + a - 2bN \right) \lambda_1 - bS\lambda_2 - kS^2 \lambda_3 = \mu_1 (N^* - N), \tag{44}$$

$$\lambda_{2_y} - \frac{2}{y} \lambda_2 - \frac{N_y}{S} \lambda_1 = 0, \tag{45}$$

$$\lambda_{3_{yy}} - \frac{2}{y} \lambda_{3_y} + \left(\frac{2}{y^2} - \frac{\partial k}{\partial C} NS^2 \right) \lambda_3 - \frac{\partial b}{\partial C} NS\lambda_2 - N \left(\frac{\partial a}{\partial C} - \frac{\partial b}{\partial C} N \right) \lambda_1 = 0, \tag{46}$$

$$\lambda_1(y,T) = 0, \tag{47}$$

$$\lambda_2(1,t) = -\lambda_4(t), \tag{48}$$

$$\lambda_{3_y}(0,t) = 0, \tag{49}$$

$$\lambda_3(1,t) = 0, \tag{50}$$

$$\lambda_{4_t}(t) = \int_0^1 \left(\frac{N_y V}{S^2} \lambda_1 - \frac{y}{S} \frac{\partial}{\partial t} (N_y \lambda_1) + bN\lambda_2 + 2kNS\lambda_3 \right) dy + \mu_2 (S^*(t) - S(t)), \tag{51}$$

$$\lambda_4(T) = -\int_0^1 \frac{N_y(y,T)\lambda_1(y,T)}{S(T)} y dy, \tag{52}$$

$$\lambda_5(t) = \lambda_2(0,t),$$

$$\lambda_6(t) = \lambda_{3_y}(1,t) - 2\lambda_3(1,t),$$

$$\lambda_7(t) = 3\lambda_3(0,t),$$

$$\lambda_8(y) = \lambda_1(y,0),$$

$$\lambda_9 = -\int_0^1 \frac{yN_y(y,0)\lambda_1(y,0)}{S(0)} dy - \lambda_4(0).$$

The above equations shall be solved in order to get λ. Notice that the adjoint equations are posed backwards in time, with a final condition at $t = T$, while the state equations are posed forward in time, with an initial condition at $t = 0$.

Now, we can obtain an expression for $\tilde{J}'(p)$ by using (30). Since $\frac{\partial J}{\partial p}(\phi, p) = 0$ and $\left(\frac{\partial E}{\partial p}(\phi, p) \right)^* \lambda \in \mathbb{R}^3$, we obtain the following expressions

$$\frac{\partial \tilde{J}}{\partial c_c}(p) = \iint_\Omega \left[\frac{C}{(C + c_c)^2} N(1-N)\lambda_1 + \frac{C}{(C + c_c)^2} NS\lambda_2 + \frac{\widehat{\beta} C}{(C + c_c)^2} NS^2 \lambda_3 \right] dt dy,$$

$$\frac{\partial \tilde{J}}{\partial c_d}(p) = \iint_\Omega \left[\frac{\sigma BC}{A(C + c_d)^2} N(1 - (1-\delta)N)\lambda_1 + \frac{\sigma BC}{A(C + c_d)^2} (1-\delta) NS\lambda_2 \right] dt dy,$$

$$\frac{\partial \tilde{J}}{\partial \sigma}(p) = \iint_\Omega \left[\frac{BC}{A(C + c_d)} N((1-\delta)N - 1)\lambda_1 - \frac{BC}{A(C + c_d)} (1-\delta) NS\lambda_2 \right] dt dy.$$

5. Resolution of the adjoint and reduced problems

5.1. Designing an algorithm to solve the adjoint problem

It is worth stressing that obtaining model parameters via minimization of the objective function $\tilde{J}$ is in general an iterative process requiring the value of the derivative. To compute $\tilde{J}'$ we just solve two systems of PDEs per iteration: the direct and

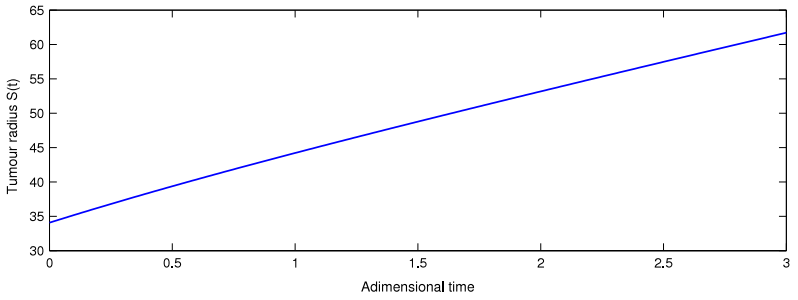

Fig. 2. Evolution of the tumor radius in time.

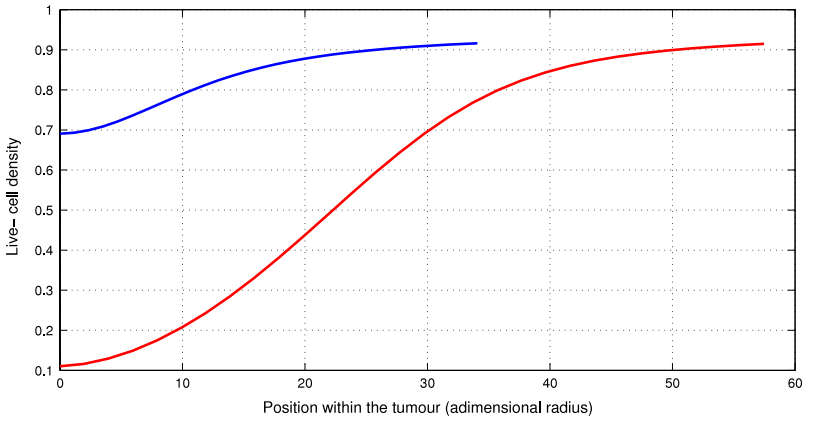

Fig. 3. Live-cell density within the tumor for two different times. Blue (upper) line corresponds to $t = 0$ and red (bottom) line corresponds to $t = 2.5$. Note that from $t = 0$ to $t = 2.5$ the tumor has also grown in size. (For interpretation of the references to colour in this figure legend, the reader is referred to the web version of this article.)

the adjoint problems. This method is much cheaper than the sensitivity approach [37] in which the direct problem is solved many times per iteration. We developed an implementation in Fortran 2003 using an object-oriented strategy (with Fortran Intel Compiler 12.0.3). In order to solve the adjoint problem we need to solve first the direct problem. Fig. 2 shows the evolution of the tumor radius in time, and Fig. 3 represents the living cell density within the tumor for two different times.

Although the adjoint problem is quite similar to the direct one, its resolution involves more difficulties. For example, there is no explicit boundary condition for λ_2. In our particular case, it is not necessary to compute $\{\lambda_i\}_{i=4}^{9}$ in order to calculate the derivative of $\tilde{J}$ with respect to p, because $\{E_i\}_{i=4}^{9}$ does not depend on the parameters p (see Eqs. (23) and (30)). However, λ_4 is required since it gives us the boundary condition for λ_2 (see Eq. (48)). Notice that an explicit expression for λ_4 can be obtained from Eq. (51).

To design a numerical procedure we perform the following steps at time T:

- Eq. (47) states that $\lambda_1(\cdot, T) = 0$.
- By Eq. (52) we have that $\lambda_4(T) = 0$, which gives us a boundary condition for λ_2 (see Eq. (48)).
- Eq. (45) can be solved analytically getting $\lambda_2(\cdot, T) = 0$.
- Eqs. (46), (49) and (50) allows us to obtain $\lambda_3(\cdot, T)$.

Knowing the solution at time t, we obtain the solution at time $t - \Delta t$ in the following way:

- By Eq. (44) we first obtain $\lambda_{1t}(\cdot, t)$. Then we get $\lambda_1(\cdot, t - \Delta t)$ using a backward finite difference.
- Using Eq. (51), we integrate numerically to obtain $\lambda_{4t}(t)$ and then we get $\lambda_4(t - \Delta t)$ by means of backward finite differences.
- With the value of $\lambda_4(t - \Delta t)$ we obtain $\lambda_2(1, t - \Delta t)$ via Eq. (48).
- Eq. (45) can be solved numerically to get $\lambda_2(\cdot, t - \Delta t)$.
- Solving Eqs. (46), (49) and (50) we obtain $\lambda_3(\cdot, t - \Delta t)$.

As well as in the direct problem, in the adjoint one we have to be careful with the singularities in the PDEs. For example, if we take a look at Eq. (46) together with the boundary conditions (49) and (50), for a fixed time t, we can ask ourselves about the solvability of this problem around $y = 0$. However, there is a difference between the direct and the adjoint problems regarding the kind of singularities that Eqs. (12) and (46) have in the origin.

The second term in (46), for instance, looks harmless because $\lambda_{3y}(0, t) = 0$ by (49), so upon expanding λ_{3y} by Taylor about 0 and dividing by y, the singularity disappears. On the other hand, the problem with the third term is harder, because

we get a blowup in the origin. To solve this problem we transform Eqs. (46), (49) and (50) into a first order ODE for a fixed time t, namely:

$$\begin{bmatrix} u \\ v \end{bmatrix}' = \begin{bmatrix} \dfrac{2}{y}v - \left(\dfrac{2}{y^2} - NS^2\dfrac{\partial k}{\partial C}\right)u - \left(N^2\dfrac{\partial b}{\partial C} - N\dfrac{\partial a}{\partial C}\right)\lambda_1 + NS\dfrac{\partial b}{\partial C}\lambda_2 \end{bmatrix}, \tag{53}$$

$$u(1) = 0, \tag{54}$$

$$v(0) = 0, \tag{55}$$

where $u(y) = \lambda_3(y, t)$ and $v(y) = \lambda_{3y}(y, t)$. Then, for a fixed $\epsilon > 0$ we propose a parameter $q = v(1)$, and solve the system (53)–(55) in the interval $[\epsilon, 1]$ with boundary conditions $u(1) = 0$ and $v(1) = q$, obtaining a solution $[u_q, v_q]^T$. Using Taylor expansions near $y = 0$ we extend these solutions to the whole interval $[0, 1]$ (see [38]).

$$u_q(0) \approx u_q(\epsilon) - \epsilon u_q'(\epsilon), \tag{56}$$

$$v_q(0) \approx v_q(\epsilon) - \epsilon v_q'(\epsilon). \tag{57}$$

The next step is to define a function

$$F(q) = v_q(0), \tag{58}$$

and to find a root of F, i.e., to find $\hat{q}$ such that $F(\hat{q}) = 0$. Then, the solution of the system will be $[u_{\hat{q}}, v_{\hat{q}}]^T$ extended to the interval $[0, 1]$.

To solve the first order ODE (45) for $\lambda_2(\cdot, t)$ with boundary condition $\lambda_2(1, t)$ known from (48), we also solve the problem in the interval $[\epsilon, 1]$ and then extend the solution to the interval $[0, 1]$ using a first order Taylor expansion.

In general, the derivatives that appear in the adjoint system of PDEs are approximated using a finite difference scheme. For example, in order to solve Eq. (44) we consider

$$\lambda_1(y, t - \Delta t) \approx \lambda_1(y, t) - \lambda_{1t}(y, t)\Delta t,$$

and using (44) we get

$$\begin{aligned} \lambda_1(y, t - \Delta t) \approx\ & \lambda_1(y, t) + \Delta t\frac{V(y, t) - yS'(t)}{S(t)}\lambda_{1y} \\ & + \Delta t\left(\frac{V_y(y, t) - S'(t)}{S(t)} + a(C(y, t)) - 2b(C(y, t))N(y, t)\right)\lambda_1(y, t) \\ & + \Delta t\left[b(C(y, t))S(t)\lambda_2(y, t) + k(C(y, t))S(t)^2\lambda_3(y, t) + \mu_1(N^*(y, t) - N(y, t))\right]. \end{aligned}$$

Notice that we are now able to obtain the solution of the adjoint problem in terms of the solution of the direct problem (the vector $\phi = [N, V, C, S]^T$), i.e. the vector λ, and that will let us compute the derivative of the objective function, as we show in the following subsection. This derivative must be used to design any gradient-based optimization method.

5.2. Optimization

It is well-known [39] that gradient-based optimization algorithms require the evaluation of the gradient of the functional, and besides that, nonheuristic optimization is based on gradient-related algorithms [40]. One important advantage of evaluating the gradient through adjoints is that it requires to solve the adjoint problem only once per iteration, regardless the number of inversion variables. Note that the derivative of the functional can be approximated by using finite differences, but this is an expensive approach because it needs, for each optimization iteration, to solve the direct problem as many times as the number of inversion variables.

The method we will use for minimizing the functional $\tilde{J}$ can be summarized as follows:

Algorithm 5.1 (*Adjoint-Based Minimization Method*)**.**

1. Give an initial guess p^0 for the vector of parameters.
2. Given the vector p^k in step k, solve the direct and adjoint problems at this step.
3. Obtain the derivative of the functional, i.e. $\tilde{J}'(p^k)$, using (30).
4. Move in the direction of $-\tilde{J}'(p^k)$, i.e., compute $p^{k+1} = \Pi_{U_{\text{ad}}}\left[p^k - \alpha\tilde{J}'(p^k)\right]$, where α is a positive parameter to be chosen, and $\Pi_{U_{\text{ad}}}$ denotes the projection on the set of admissible points.
5. Stop when $\tilde{J}\left(p^{k+1}\right)$ is less than a tolerance $TOL_1 > 0$, or when the distance between two consecutive iterations is less than a tolerance $TOL_2 > 0$, that is, $\|p^{k+1} - p^k\| < TOL_2$.

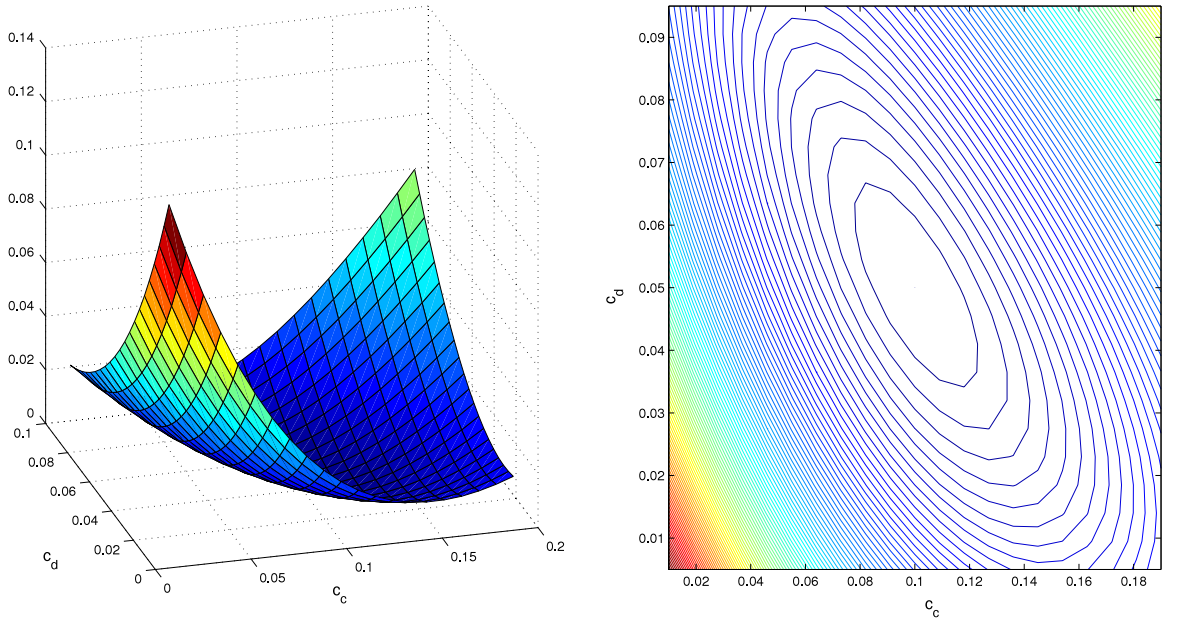

Fig. 4. Functional value of J (22) in terms of c_c and c_d for constant $\sigma = 0.9$. Note that the surface reaches a minimum near $c_c = 0.1$ and $c_d = 0.05$.

6. Numerical experiments

The goal of this section is to test and evaluate the performance of an adjoint-based optimization method, by executing some numerical simulations of Algorithm 5.1 for some test-cases.

We took a spatial grid consisting of 31 equidistant points $0 = y_0 < \cdots < y_{30} = 1$, and a temporal grid t_k consisting of steps of length 0.01.

In order to perform Step 2 of Algorithm 5.1, for a given vector of parameters p^k, we solve the direct problem from $t = -4.5$ up to $t = T$ where $T = 0.5$. This means that the tumor is first detected at time $t = 0$, by which time it has grown following the model [16]: originally, at an adimensional time $t = -4.5$, a single cell started to take nutrients from the environment, letting it grow up to a dimensionless size S_l and a living cell density N_l. One example for the initial profile N_l could be the blue line in Fig. 3. After solving the direct problem, the adjoint problem is solved following the procedure explained in Section 5.1.

To compute the derivative of the functional J, Step 3 of Algorithm 5.1, we use Eq. (30). To work with functional (22), it is necessary to have the measurements at each t_k (by interpolating if necessary). For simplicity, we approximate the integral by a quadrature using the spatial and temporal grids (y_l, t_k). The factors μ_1 and μ_2 are taken to be 100 and 1 respectively (to scale the two terms in (22)), and the parameter α used in the projection over the admissible set is taken to be 0.1.

6.1. Model-generated data

Consider first an optimization problem that consists in minimizing the functional (22), where $N^*(y, t)$ and $S^*(t)$ are generated by solving the direct problem, for a choice of the model parameters $c_c = 0.1$, $c_d = 0.05$, $\sigma = 0.9$ as suggested in [16].

Fig. 4 shows the value that the functional (22) takes for different values of c_c and c_d, remaining σ as a constant equal to 0.9. It is worth mentioning that J looks convex and that the variations are greater with respect to c_c compared to those with respect to c_d.

The idea of this test case is to investigate how close the original value of the parameter can be retrieved. However, it is not a trivial one, because we cannot prove analytically if the optimization problem has a solution or, in that case, if it is unique or if the method converges to another local minima.

We emphasize that we have run the algorithm several times using different initial points and in all cases the results had relative errors of the same order. They can be summarized as:

- Stopping criteria: $TOL_1 = 10^{-6}$ or $TOL_2 = 10^{-6}$
- Iterations/elapsed time: 140 iterations in 12.7 min
- Initial point: $p_0 = [0.16, 0.03, 1.0]$
- Final point: $p_f = [0.1006492, 0.084465653, 0.9297853]$
- Functional final value: $J(p_f) = 0.991496220 \times 10^{-6}$

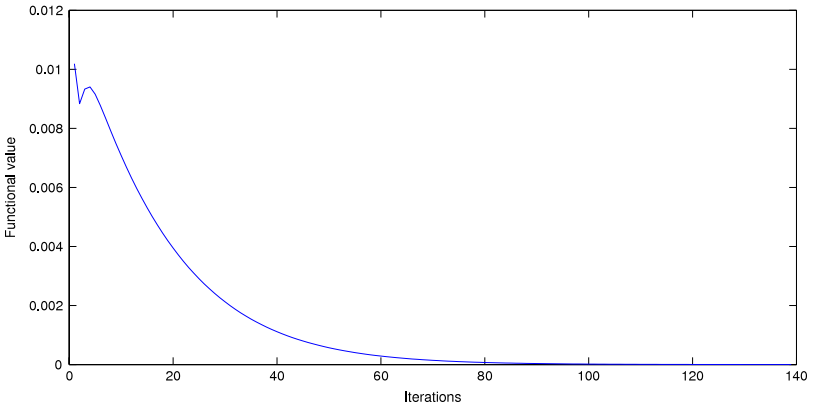

Fig. 5. Evolution of the functional value of J (22) with the number of iterations.

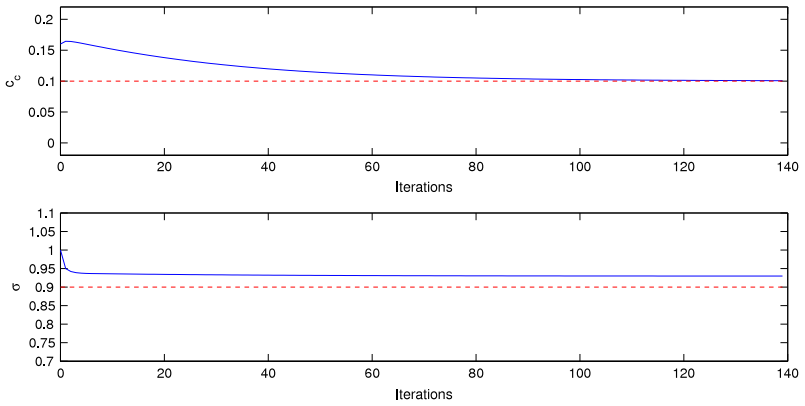

Fig. 6. Evolution of the c_c and σ values with the number of iterations (solid lines) and *real values* of c_c and σ (dashed lines).

- Relative error of the initial point: 60% for c_c, 40% for c_d, 11.11% for σ,
- Relative error of the final point: 0.6492% for c_c, 68.9313% for c_d, 3.3095% for σ.

Fig. 5 represents the evolution in the value of J with the number of iterations. Fig. 6 shows the evolution of c_c and σ respectively, and the *real value* of this parameters. Due to the flatness of the functional J with respect to c_d, the relative error at the final point has the same magnitude of the relative error at the initial point. Thus, we have not included the evolution of c_d in Fig. 6.

The Algorithm 5.1 stops because the functional reaches values less than TOL_1.

6.2. Model-generated data with Gaussian random noise

It is well known that the presence of noise in the data may imply the appearance of strong numerical instabilities in the solution of an inverse problem [41].

The outputs of the detectors and experimental equipments where the variables N^* and S^* are measured are often affected by perturbations, usually random ones. As stated in [23], it is in general valid to consider a 5% of Gaussian random noise.

After running the algorithm several times using different initial points, the obtained results had relative errors of the same order. They can be summarized as:

- Stopping criteria: $TOL_1 = 10^{-6}$ or $TOL_2 = 10^{-6}$
- Iterations/elapsed time: 143 iterations in 13 min
- Initial point: $p_0 = [0.16, 0.03, 1.0]$
- Final point: $p_f = [0.1592, 0.0481, 0.9811]$
- Functional final value: $J(p_f) = 0.01830000000$
- Relative error of the initial point: 60% for c_c, 40% for c_d, 11.11% for σ,
- Relative error of the final point: 3.3045% for c_c, 33.6894% for c_d, 6.8348% for σ.

Fig. 7 shows the value that the functional (22) takes for different values of c_c and c_d, remaining σ as a constant and assuming that S^* and N^* are obtained with 5% of Gaussian random noise.

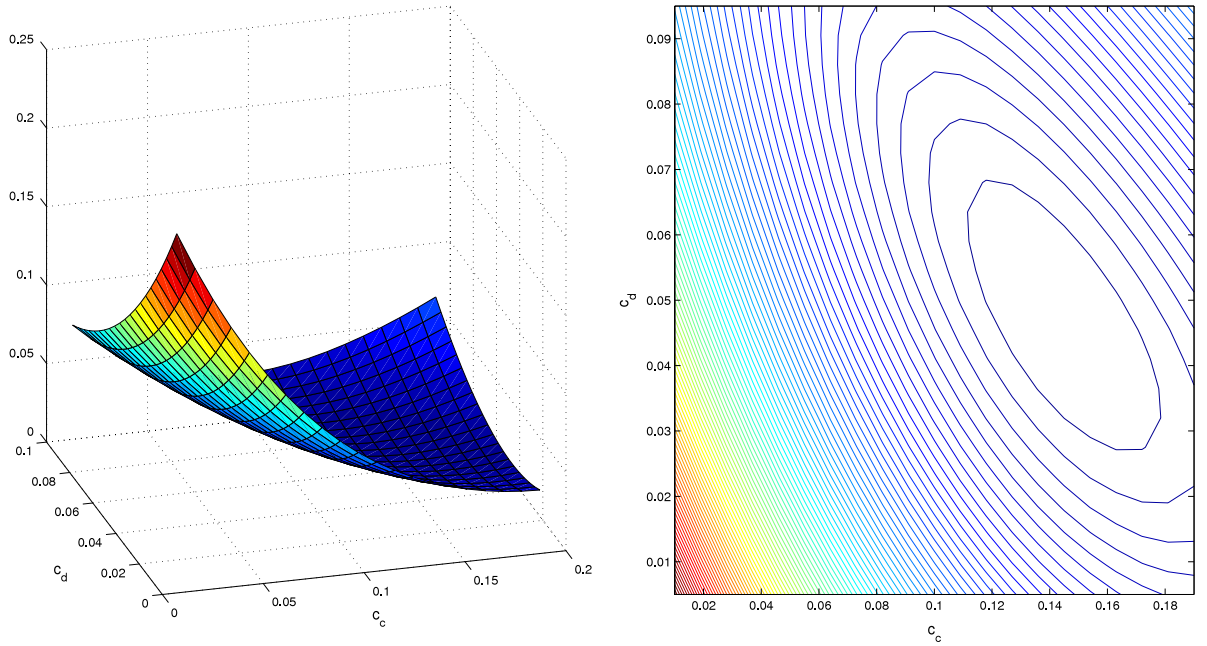

Fig. 7. Functional value of J (22) in terms of c_c and c_d for constant $\sigma = 0.9$, for data with 5% of Gaussian random noise.

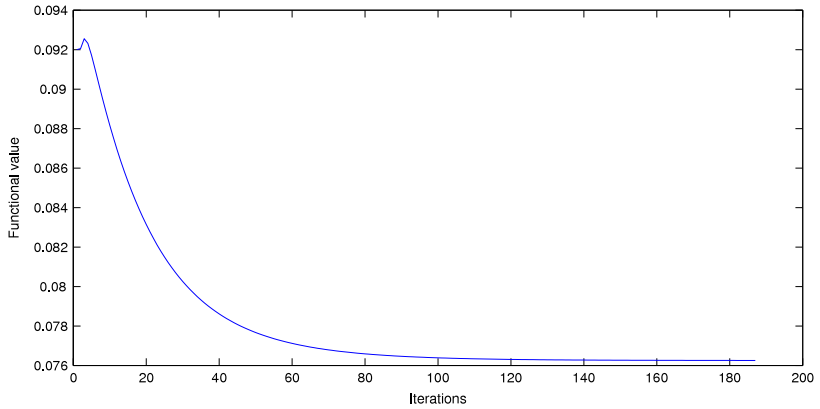

Fig. 8. Evolution of the functional value with the number of iterations, for data with 5% of Gaussian random noise.

Fig. 8 represents the evolution in the value of J with the number of iterations. A comparison with Fig. 5 shows that the functional values are greater in this case, but the algorithm stops because the variations become small. Fig. 9 shows the evolution of c_c and the *real value* of this parameter.

We can choose one of the variables considered in the functional (22) and look for difference between the real value of this variable and the value that corresponds to the solution of the direct problem for the parameters obtained after running the algorithm.

The case in which we considered model-generated data with 5% of Gaussian random noise is, as expected, not as precise as the case in which the data is generated without noise. The Algorithm 5.1 stops by a different reason because the difference between two consecutive iterates is less than TOL_2.

7. Conclusions

The scientific community agrees that life's sciences, like biology or medicine, need the development of new tools in order to build models able to reproduce and to predict real phenomena. Over the last decades, a number of mathematical models for cancer onset and growth have been proposed [27,5], and it became clear that these models are expected to success if the parameters involved in the modeling process are known. Or eventually, taking into account that some biological parameters may be unknown (especially *in vivo*), the model can be used to obtain them [23,21].

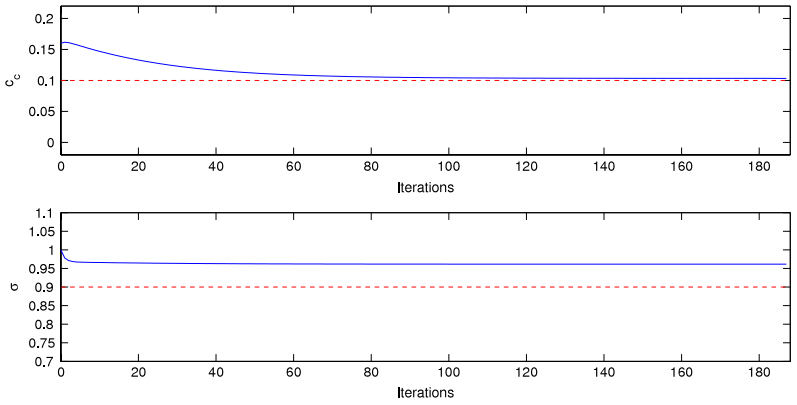

Fig. 9. Evolution of the c_c and σ values with the number of iterations (solid lines) for data with 5% of Gaussian random noise and *real values* of c_c and σ (dashed line).

This paper, as already mentioned in Section 1, aims at offering a mathematical tool for the obtention of phenomenological parameters which can be identified by inverse estimation, by making suitable comparisons with experimental data. The inverse problem, which was stated as a PDE-constrained optimization problem, has been solved by using the adjoint method, which has shown to work efficiently. In addition, the gradient of the proposed functional is obtained and the methodology can be extended, in principle, to any number of unknown parameters.

Focusing on further developments of the mathematical tools, it is worth mentioning that the numerical resolution proposed in this paper is in some aspects challenging and several numerical procedures were introduced in order to deal with non-linearities and singularities in the adjoint system of PDEs.

There already exist in the literature some other works which focus on parameter estimation via resolution of the adjoint problem, for instance the paper by Hogea et al. [13]. However, for the best of our knowledge, this is the first time that this technique has been applied to a free boundary model for tumor growth.

In addition, we remark that the parameter estimation via PDE-constrained optimization is a general approach that can be used, for instance, to consider the effects of chemotherapy. We are currently working in this line and also in the resolution of the optimization problem but after discretizing the original system of PDEs, in order to compare and contrast the performance of both methods.

Acknowledgements

We appreciate the courtesy of Milena Batalla and Lucia Policastro, from the *Grupo de Micro y Nanotecnología – Gerencia de Área de Investigaciones y Aplicaciones No Nucleares — CNEA Argentina*, who strongly contributed with information and motivations for this work.

We also thank the anonymous referees for their valuable contributions to our manuscript.

The work of the authors was partially supported by grants from CONICET, SECYT-UNC and PICT-FONCYT.

References

[1] E.L. Bearer, J.S. Lowengrub, H.B. Frieboes, Y.L. Chuang, F. Jin, S.M. Wise, M. Ferrari, D.B. Agus, V. Cristini, Multiparameter computational modeling of tumor invasion, Cancer Research 69 (10) (2009) 4493–4501.
[2] J.T. Oden, A. Hawkins, S. Prudhomme, General diffuse-interface theories and an approach to predictive tumor growth modeling, Mathematical Models and Methods in Applied Sciences 20 (03) (2010) 477–517.
[3] N. Bellomo, A. Bellouquid, J. Nieto, J. Soler, Multiscale biological tissue models and flux-limited chemotaxis for multicellular growing systems, Mathematical Models and Methods in Applied Sciences 20 (07) (2010) 1179–1207.
[4] N. Bellomo, A. Bellouquid, J. Nieto, J. Soler, On the asymptotic theory from microscopic to macroscopic growing tissue models: an overview with perspectives, Mathematical Models and Methods in Applied Sciences 22 (01) (2012).
[5] N. Bellomo, N.K. Li, P.K. Maini, On the foundations of cancer modelling: selected topics, speculations, and perspectives, Mathematical Models and Methods in Applied Sciences 18 (04) (2008) 593–646.
[6] K.A. Rejniak, L.J. McCawley, Current trends in mathematical modeling of tumor–microenvironment interactions: a survey of tools and applications, Experimental Biology and Medicine 235 (4) (2010) 411–423.
[7] L. Preziosi, G. Vitale, A multiphase model of tumor and tissue growth including cell adhesion and plastic reorganization, Mathematical Models and Methods in Applied Sciences 21 (09) (2011) 1901–1932.
[8] M. Scianna, L. Preziosi, A hybrid model describing different morphologies of tumor invasion fronts, Mathematical Modelling of Natural Phenomena 7 (01) (2012) 78–104.
[9] S.M. Wise, J.S. Lowengrub, H.B. Frieboes, V. Cristini, Three-dimensional multispecies nonlinear tumor growth-I: model and numerical method, Journal of Theoretical Biology 253 (3) (2008) 524–543.
[10] H.P. Greenspan, Models for the growth of a solid tumor by diffusion, Studies in Applied Mathematics 51 (4) (1972) 317–340.
[11] R.M. Shymko, L. Glass, Cellular and geometric control of tissue growth and mitotic instability, Journal of Theoretical Biology 63 (2) (1976) 355–374.

[12] G.A. Santa Cruz, S.J. González, A. Dagrosa, A.E. Schwint, M. Carpano, V.A. Trivillin, E.F. Boggio, J. Bertotti, J. Marín, A. Monti Hughes, A.J. Molinari, M. Albero, Dynamic infrared imaging for biological and medical applications in boron neutron capture therapy, in: Thermosense: Thermal Infrared Applications XXXIII, Vol. 8013, 2011.
[13] C. Hogea, C. Davatzikos, G. Biros, An image-driven parameter estimation problem for a reaction–diffusion glioma growth model with mass effects, Journal of Mathematical Biology 56 (6) (2008) 793–825.
[14] H.M. Byrne, M.A.J. Chaplain, Free boundary value problems associated with the growth and development of multicellular spheroids, European Journal of Applied Mathematics 8 (06) (1997) 639–658.
[15] J. Crank, Free and Moving Boundary Problems, Oxford Science Publications, The Clarendon Press, Oxford University Press, New York, 1984.
[16] J.P. Ward, J.R. King, Mathematical modelling of avascular-tumour growth, Mathematical Medicine and Biology 14 (1) (1997) 39–69.
[17] J.P. Ward, J.R. King, Mathematical modelling of drug transport in tumour multicell spheroids and monolayer cultures, Mathematical Biosciences 181 (2) (2003) 177–207.
[18] R. Venkatasubramanian, M.A. Henson, N.S. Forbes, Incorporating energy metabolism into a growth model of multicellular tumor spheroids, Journal of Theoretical Biology 242 (2) (2006) 440–453.
[19] A. Bertuzzi, A. Fasano, A. Gandolfi, C. Sinisgalli, ATP production and necrosis formation in a tumour spheroid model, Mathematical Modelling of Natural Phenomena 2 (3) (2007) 30–46.
[20] B. Perthame, J.P. Zubelli, On the inverse problem for a size-structured population model, Inverse Problems 23 (3) (2007) 1037–1052.
[21] K. van den Doel, U.M. Ascher, D.K. Pai, Source localization in electromyography using the inverse potential problem, Inverse Problems 27 (2) (2011) 025008. 20.
[22] J.P. Zubelli, R. Marabini, C.O.S. Sorzano, G.T. Herman, Three-dimensional reconstruction by chahine's method from electron microscopic projections corrupted by instrumental aberrations, Inverse Problems 19 (4) (2003) 933–949.
[23] J.P. Agnelli, A.A. Barrea, C.V. Turner, Tumor location and parameter estimation by thermography, Mathematical and Computer Modelling 53 (7–8) (2011) 1527–1534.
[24] D.A. Knopoff, D.R. Fernández, G.A. Torres, C.V. Turner, A mathematical method for parameter estimation in a tumor growth model, 2012, submitted for publication.
[25] R.P. Araujo, D.L.S. McElwain, A history of the study of solid tumour growth: the contribution of mathematical modelling, Bulletin of Mathematical Biology 66 (5) (2004) 1039–1091.
[26] J.A. Adam, A simplified mathematical model of tumor growth, Mathematical Biosciences 81 (2) (1986) 229–244.
[27] J.A. Adam, N. Bellomo, A survey of models for tumor immune systems dynamics, in: Modeling and Simulation in Science, Engineering & Technology, Birkhäuser, 1997.
[28] D.L. Taylor, A.S. Waggoner, F. Lanni, R.F. Murphy, R.R. Birge, Applications of Fluorescence in the Biomedical Sciences, 1986.
[29] G.R. Martin, R.K. Jain, Noninvasive measurement of interstitial pH profiles in normal and neoplastic tissue using fluorescence ratio imaging microscopy, Cancer Research 54 (21) (1994) 5670–5674.
[30] J.P. Freyer, R.M. Sutherland, Regulation of growth saturation and development of necrosis in EMT6/Ro multicellular spheroids by the glucose and oxygen supply, Cancer Research 46 (7) (1986) 3504–3512.
[31] A. Monazzam, R. Josephsson, C. Blomqvist, J. Carlsson, B. Långström, M. Bergström, Application of the multicellular tumour spheroid model to screen PET tracers for analysis of early response of chemotherapy in breast cancer, Breast Cancer Research 9 (2007) R45.
[32] M. Bergström, A. Monazzam, P. Razifar, S. Ide, R. Josephsson, B. Långström, Modeling spheroid growth, PET tracer uptake, and treatment effects of the Hsp90 inhibitor NVP-AUY922, Journal of Nuclear Medicine 49 (7) (2008) 1204–1210.
[33] R. Herrmann, W. Fayad, S. Schwarz, M. Berndtsson, S. Linder, Screening for compounds that induce apoptosis of cancer cells grown as multicellular spheroids, Journal of Biomolecular Screening 13 (1) (2008) 1–8.
[34] H.W. Engl, M. Hanke, A. Neubauer, Regularization of Inverse Problems, in: Mathematics and its Applications, vol. 375, Kluwer Academic Publishers Group, Dordrecht, 1996.
[35] A. Kirsch, An Introduction to the Mathematical Theory of Inverse Problems, in: Applied Mathematical Sciences, vol. 120, Springer-Verlag, New York, 1996.
[36] C. Brandenburg, F. Lindemann, M. Ulbrich, S. Ulbrich, A continuous adjoint approach to shape optimization for Navier Stokes flow, in: Optimal Control of Coupled Systems of Partial Differential Equations, in: Internat. Ser. Numer. Math., vol. 158, Birkhäuser Verlag, Basel, 2009, pp. 35–56.
[37] M. Hinze, R. Pinnau, M. Ulbrich, S. Ulbrich, Optimization with PDE Constraints, in: Mathematical Modelling: Theory and Applications, vol. 23, Springer, New York, 2009.
[38] U.M. Ascher, R.M.M. Mattheij, R.D. Russell, Numerical Solution of Boundary Value Problems for Ordinary Differential Equations, in: Classics in Applied Mathematics, vol. 13, Society for Industrial and Applied Mathematics (SIAM), Philadelphia, PA, 1995, Corrected reprint of the 1988 original.
[39] J. Nocedal, S.J. Wright, Numerical Optimization, in: Springer Series in Operations Research, Springer-Verlag, New York, 1999.
[40] D.P. Bertsekas, Nonlinear Programming, 1999.
[41] M. Bertero, M. Piana, Inverse problems in biomedical imaging: modeling and methods of solution, Complex Systems in Biomedicine (2006) 1–33.